JOURNAL OF MATERIALS SCIENCE 36 (2001) 5169–5175

Evaluation of time-dependent change in fiber stress profiles during long-term pull-out tests at constant loads using Raman spectroscopy

T. MIYAKE
Nagoya Municipal Industrial Research Institute, 3-4-41, Rokuban, Atsuta-ku, Nagoya 456-0058, Japan
E-mail: miyake@nmiri.city.nagoya.jp

S. KOKAWA, N. OHNO, S. BIWA
Department of Micro System Engineering, Nagoya University, Furo-cho, Chikusa-ku, Nagoya 464-8603, Japan

Constant-load pull-out tests were carried out on single-fiber model composite specimens for 500 to 1,000 hours in order to investigate the time-dependent change in fiber axial stress profiles resulting from matrix creep in unidirectional continuous fiber-reinforced composites. Three resins used as the matrix materials, in which single carbon fibers were embedded, were normal epoxy, a blend with a more flexible epoxy, and UV-curable acrylic. The time-dependent change in fiber stress profiles in the constant-load pull-out tests was measured using Raman spectroscopy, and creep and relaxation tests for the matrix resins themselves were performed. It was observed that the normal epoxy matrix composite exhibited only a negligible change in the fiber stress profile with time whereas the flexible epoxy and UV-curable acrylic matrices allowed, respectively, considerable and significant changes. These observations were shown to be consistent with the creep and stress relaxation test results of the matrix resins. It was also found that the time-dependent change in fiber stress was much slower in the experiment than in the prediction based on perfect bonding at the fiber/matrix interface. The interfacial slip that occurred in the composites tested could be responsible for the gradual variation in fiber stress profiles.

1. Introduction

Unidirectional composites reinforced with long continuous fibers often suffer from fiber breakage. In a broken fiber, the axial stress diminishes at the break and builds to those stresses in intact fibers a certain distance away. Such a distance in the broken fiber where the axial stress varies is referred to as the stress recovery length, and plays a substantial role in the strength characteristics of composites. This is especially so regarding the long-term failure behavior of composites such as creep.

As the matrix undergoes shear creep in the neighborhood of a fiber break, the stress recovery length of the fiber increases with time, so that the load carried by the broken fiber is reduced. As a consequence, creep failure can occur even under constant loading applied in the fiber direction. This has motivated several investigations from theoretical viewpoints regarding the time-dependent change in stress profiles of broken fibers [1–9]. These studies have revealed that the stress recovery length grows with time as the matrix creeps, but different assumptions employed by different authors have yielded divergent predictions. For instance, on the basis of perfect bonding at the fiber/matrix interface, the stress recovery length is found to increase rapidly after fiber breakage [1, 4, 5]. On the other hand, the evolution of this length turns out to be quite slow when incipient slippage at the fiber/matrix interface is accounted for [7, 9].

When it comes to experimental aspects of the above subject, an investigation was made by the present authors concerning the time-dependent change in stress profiles of broken fibers using Raman spectroscopy [10]. Single-carbon-fiber/epoxy model composites were employed. Each specimen was subjected to tensile elongation until the fiber first broke, and the stress profile of the broken fiber was then measured for 1,000 hours with the tensile strain of the composite kept constant. This experiment showed that the temporal change in the stress recovery length of broken fibers is not significant, despite the fact that the matrix itself exhibits notable stress relaxation. Another Raman spectroscopic investigation on creep was made for carbon fiber/polypropylene model composites [11]. That work, however, involved short-fiber-reinforced composites, where the load transfer between the fiber and the matrix

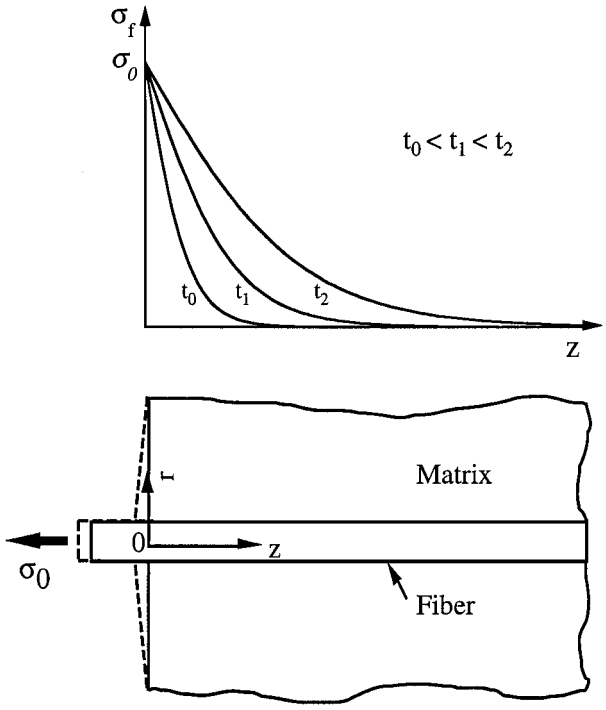

Figure 1 Time-dependent change in fiber stress profiles in constant-load pull-out tests.

was found to be entirely frictional in character. No other experimental findings are available on this issue, which highlights the necessity to carry out further experimental studies of different material systems or under a range of environmental conditions in order to clarify the influence of matrix creep on the stress profiles of broken fibers.

Time-dependent change in fiber stress profiles similar to those in broken fibers can occur in fiber pull-out tests where the pull-out loads are kept constant. In the pull-out tests, due to the shear stress at fiber/matrix interface, the surrounding matrix undergoes shear creep. This causes the axial distribution of fiber stress to change with time t as depicted in Fig. 1. Accordingly, the stress transfer length (a length scale corresponding to the stress recovery length and represented by the distance over which σ_f decays from the pull-out stress σ_0 to zero) increases with time. In fact, the time variations in fiber stress profiles in both tests can be described in the same manner if the shear-lag assumption is employed [5]. Moreover, constant-load pull-out tests have certain advantages over the stress relaxation tests for composites with fiber breakage reported previously [10], since in the pull-out tests merely dead loads need to be applied to fiber ends.

The objective of the present study is to investigate the time evolution of the stress transfer length in constant-load pull-out specimens by Raman spectroscopy. Three types of resins with different creep properties are employed as the matrix to elucidate the influence of creeping behavior. Although the application of Raman spectroscopy to single-fiber pull-out tests was reported earlier by Patrikis *et al*. [12] and Gu *et al*. [13], these works were confined to the change in fiber stress profiles with increased pull-out loads. In the present work, the time-dependent variation in stress profiles of fibers embedded in creeping matrices is examined in detail.

2. Experimental procedure

2.1. Materials

The present experiment utilized commercially available high modulus PAN-based carbon fibers (SR-40K, Mitsubishi Rayon Co., Ltd.) with Young's modulus 490 GPa and a 0.9% failure strain in average. The fibers were about 5.2 μm in diameter and subjected to a standard oxidation treatment. As the matrix, three different kinds of resins were employed, namely, (I) a common room-temperature curing bisphenol-A type resin (Epotek 301-2, Epoxy Technology, Inc.), (II) a 1 : 1 weight-ratio mixture of the above resin (I) and a more flexible one (Epotek 310, Epoxy Technology, Inc.) having a sub-ambient glass transition temperature, and (III) a UV-curable acrylic (Light-Weld 425, Dymax Corp.). Hereafter, these three resins are referred to as epoxy-1 (normal epoxy), epoxy-2 (flexible epoxy) and acrylic (UV-curable acrylic), respectively. Some of the mechanical properties of these resins as well as those of the carbon fibers are summarized in Table I.

2.2. Preparation of single-fiber pull-out specimens

Fig. 2 illustrates schematically the preparation of single-fiber pull-out specimens. A single fiber was first mounted onto a plastic frame with a window 50 mm long and of a prolonged circular shape. Transparent cover glasses were attached to both faces of the frame to make a cavity to mold a resin. Each of the resins was drawn into a syringe in a vacuum-degassed state and introduced into the cavity, where the resin was

TABLE I Mechanical properties of materials used for model composites

	Carbon fiber	Epoxy-1	Epoxy-2	Acrylic
Tensile modulus (GPa)	490[a]	3.6	1.2	1.5
Tensile strength (MPa)	4300[a]	60	20	26
Poisson's ratio	–	0.29	0.30	0.32
Elongation (%)	0.9[a]	5	9	11
Durometer hardness D	–	82	78	80

[a]Measured with polymer impregnated strands.

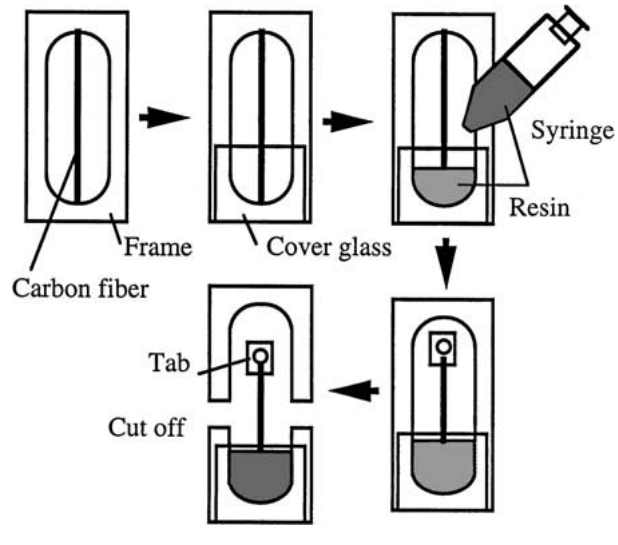

Figure 2 Preparation of pull-out test specimens.

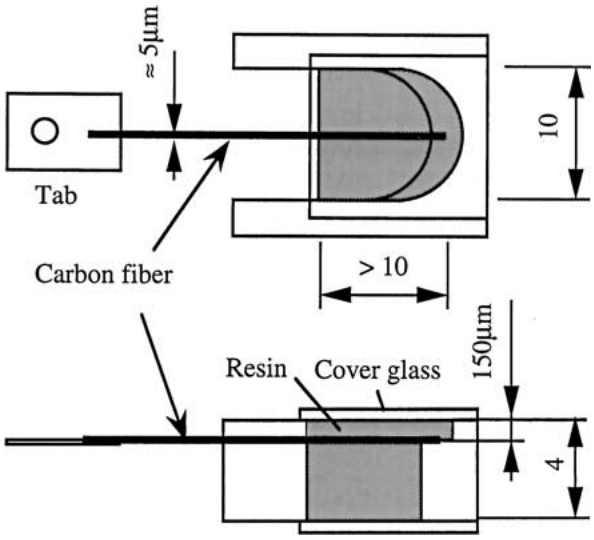

Figure 3 Shape of pull-out test specimens.

subsequently subjected to curing. After curing, the fiber was cut at a certain distance from the resin and fixed to a tab. The frame was finally split down the middle to complete a pull-out specimen.

The pull-out specimens made of epoxy-1 and epoxy-2 were cured at room temperature for 7 and 30 days, respectively. The specimen made of acrylic was exposed to a UV lump for 1 hour by means of a parabolic reflector to achieve a uniform light intensity over the resin surface. In order to avoid local shrinkage and the resulting residual stress, the UV intensity was kept to a relatively low level of 3 mW/cm^2. Durometer hardness D was measured for each resin during the cure, because saturation of this hardness value was an indication of sufficient curing. The saturated values of hardness are also listed in Table I.

The geometry and dimensions of the specimens so prepared are illustrated in Fig. 3. Raman scattering measurements of each embedded fiber were made through the upper cover glass and the surrounding resin. To prevent severe attenuation of the scattered light from the fiber, it was embedded at a depth of 150 μm, which, though quite small, was fairly large compared to the fiber diameter. Moreover, the portion of the fiber embedded in the matrix was no less than 10 mm, so that the system well approximated an infinite matrix containing a single fiber.

2.3. Long-term pull-out tests at constant loads

Each of the single fiber specimens was fixed onto a loading device, which was then placed on the stage of the optical microscope in the Raman Spectrometer described in the following section. As shown in Fig. 4, the fiber was pulled out by a thin nylon line connected to the fiber end tab, to which a dead weight was hung via a roller. Pull-out tests were carried out on the specimens with different resins for 500 to 1,000 hours in an atmospheric environment at 298 K and at a relative humidity below 50%. Table II summarizes the experimental conditions for the three specimens. The fiber diameters in Table II were determined from scanning electron microscope photographs of cross sections taken after the pull-out tests. The listed fiber stresses are those applied to the fibers in the axial direction at exposed parts outside the resins, and were about 2.5 GPa for all tests corresponding to the axial strain of 0.5%.

TABLE II Fiber pull-out conditions for three kinds of model composites

	Carbon fiber/ epoxy-1	Carbon fiber/ epoxy-2	Carbon fiber/ acrylic
Pull-out load (mN)	52.4	52.4	62.2
Fiber diameter (μm)	5.2	5.3	5.4
Fiber stress, σ_0 (GPa)	2.5	2.4	2.7
Pull-out duration (h)	500	1000	500

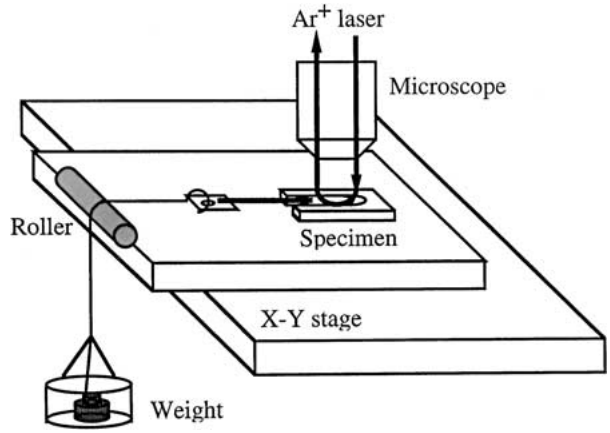

Figure 4 Schematic illustration of constant-load pull-out tests.

2.4. Raman spectroscopy measurements

Raman spectra were measured by a micro-Raman spectrometer system (SPEX-750M, Instruments S. A., Inc.) consisting of a single polychromater coupled to an optical microscope (BH-2, Olympus Optical Co., Ltd.). A 80× objective lens was used to focus the incident light of a 514.5 nm wavelength Ar^+ laser onto a 1-μm diameter spot on the fiber surface, and to collect the 180° backscattered light. The incident light intensity on the fiber surface was kept below 1 mW to avoid local overheating. The scattered light was filtered through a confocal spatial filter with a 200-μm pin hole to reduce the scattering from matrix resins. A highly sensitive charge-coupled device (CCD) cooled with liquid nitrogen was used to collect Raman spectra with an exposure of 240 seconds. Each specimen was translated in the axial direction on the X-Y stage in order to obtain Raman spectra at different axial positions. The measurements were made not only for the portion of the fiber embedded in the resin but also for the part extending outside. They were made prior to and just after the loading, and when the elapsed time reached 1, 10, 100 and 500 hours (300 hours for some specimens).

The peak position of the stress-sensitive 2700 cm^{-1} Raman band was used to evaluate the fiber stress, since the peak of the first-order 1580 cm^{-1} band was found to overlap with a Raman spectrum peak of the resins used as the matrix. The peaks were determined by a Lorentzian curve fitting procedure (LabCalc, Galiotic

Ind., Co.). A least square fitted line between the tensile stress σ_f and the peak position ν of the 2700 cm^{-1} Raman band of the carbon fibers employed reads [10]

$$\nu = 2705.0 \pm 0.2 - (7.5 \pm 0.1)\sigma_f, \qquad (1)$$

where ν and σ_f are measured in cm^{-1} and GPa, respectively. During the long-term pull-out tests, each spectrum was calibrated by a peak in a Ne spectrum to compensate for the temporal fluctuation in temperature and other conditions of the experimental system.

2.5. Creep and relaxation tests for matrix resins

As mentioned above, the time-dependent change in fiber stress profiles in pull-out tests is brought about by matrix creep driven by shear stress at the fiber/matrix interface. To characterize the long-term deformation behavior of the three resins employed in the study, creep and relaxation tests were also carried out.

Small dog-bone-shaped specimens 12 mm in gage length and 5×2 mm cross-sectional area, machined from each resin cured according to the conditions described in Section 2.2, were used in both tests. Durometer hardness D was again used to confirm that these specimens attained sufficient curing as in the model composites used in the pull-out tests.

The creep tests were performed with dead-weight loading at levels chosen to simulate the matrix shear creep in the pull-out tests as will be discussed in detail in Section 4.1 The creep strain was measured by two strain gages attached on both sides of the gage section. On the other hand, the relaxation tests were made at a prescribed strain of 0.5%. The strain was controlled by a linear actuator based on the mean output from the two strain gages, and the axial stress was monitored continuously by a load cell connected serially to the specimen.

3. Results

3.1. Pull-out tests at constant loads

Profiles of the fiber axial stress obtained by Raman spectroscopy are shown in Fig. 5a–c for the pull-out specimens with the three resins, epoxy-1, epoxy-2, and acrylic, respectively. The spatial coordinate in the axial direction is denoted by z, with the origin ($z = 0$) corresponding to the point where the fiber intersects the resin free surface and positive values of z corresponding to the inside of the resin.

For all stress profiles in Fig. 5a–c, the axial stress σ_f of fibers embedded inside resins decreases to zero with increasing distance from the origin. However, time variations in these stress profiles show some distinct features depending on the particular matrix resin. In the case of epoxy-1 shown in Fig. 5a, the stress profile appears to exhibit some variation until 1 hour after the moment of loading. Later, however, it ceases to show any notable change, and the stress recovery length retains a value of about 300 μm. For epoxy-2 in Fig. 5b, the profile also changes for up to 10 hours after loading, but with little subsequent variation. In contrast, when acrylic is employed as the matrix, as shown in Fig. 5c

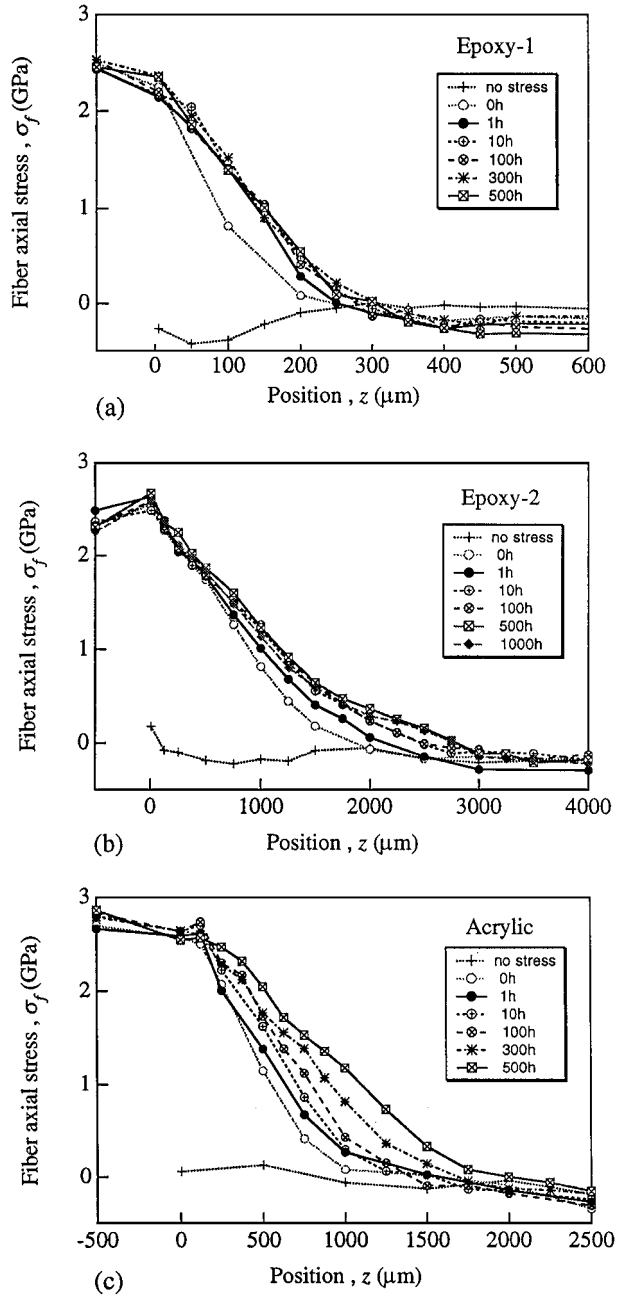

Figure 5 Profiles of fiber axial stress in pull-out test specimens for (a) epoxy-1 matrix, (b) epoxy-2 matrix, and (c) acrylic matrix.

the stress profile continuously changes as time elapses, even in a later stage between 300 and 500 hours. In particular, the stress recovery length is doubled from approximately 1,000 to 2,000 μm after 500 hours of pull-out loading, which is a trend not seen in epoxy-1 or epoxy-2. It is noted here that for Fig. 5a and b, the fiber stress outside the resin ($z < 0$) differs slightly from that at $z \approx 0$. This is considered to be due mainly to the residual stress in fibers generated during the specimen fabrication, as delineated by the '+' plots in Fig. 5a–c. It is also noted that in Fig. 5a, the fiber stress in the inner part gets compressive below the stress level obtained after curing. This might be due to slight shrinkage of the specimen with time; since Young's modulus of fibers was as high as 490 GPa, the measured variation in fiber stress at $z > 400\,\mu$m in 500 hours, which was about 0.25 GPa, could be induced if only a 0.05% shrinkage of the specimen occurred.

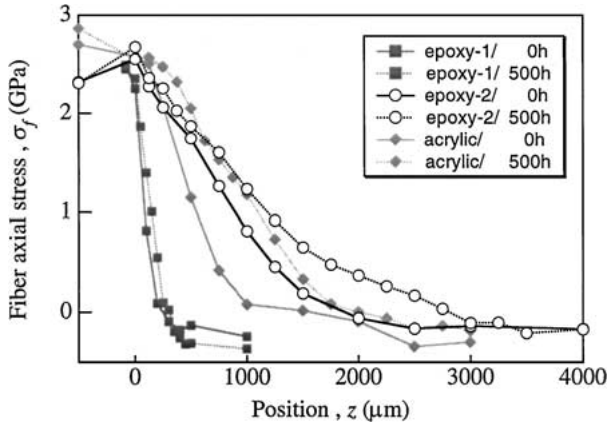

Figure 6 Comparison of the profiles of fiber axial stress in three pull-out tests at $t = 0$ hour and 500 hours.

Fig. 6 compares the profiles of fiber axial stress in the three pull-out tests at $t = 0$ hour and 500 hours. It is again seen from the figure that the time-dependent variation in fiber axial stress was little in epoxy-1 whereas it was noticeable in epoxy-2 and acrylic.

From each fiber stress distribution shown above, the interfacial shear stress τ is calculated by the following equation derived from the equilibrium of forces on the fiber element dz,

$$\tau = \frac{r_f}{2}\frac{\partial \sigma_f}{\partial z}, \tag{2}$$

where r_f denotes the fiber radius. The results are shown in Fig. 7a–c, respectively. For the numerical differentiation in Equation 2, the Savitzky-Golay smoothing procedure of five moving points was employed. As a consequence, for the two measurement points closest to the origin ($z = 0$) the interfacial shear stress was not computed.

It is observed in Fig. 7a–c that the time variation in profiles of τ depends on the resin type in a manner similar to that in axial stresses σ_f discussed previously. Namely, the degree of temporal change in shear stress profiles is more significant in the order of acrylic, epoxy-2, and epoxy-1. Particular attention is drawn here to the maximum shear stress τ_{max} at each elapsed time. This maximum value tends to decrease with time for the three specimens. Especially for the acrylic matrix, τ_{max} continues to decrease and results in roughly half the initial value after 500 hours. Moreover, for this specimen the shear stress distribution tends to approach uniformity over the region corresponding to the stress transfer length.

It is also noted here that in the results of epoxy-2 and acrylic, just after loading the shear stress profiles attain certain extrema not at $z = 0$ but at finite distances into the resins, as shown by the '○' plots in Fig. 6b and c. As further discussed in Section 4.2, this is indicative of the occurrence of interfacial slippage at initial loading.

3.2. Creep and relaxation tests for matrix resins

As already mentioned, the time-dependent change in fiber stress profiles in the constant-load pull-out tests is due to matrix creep driven by the shear stress at

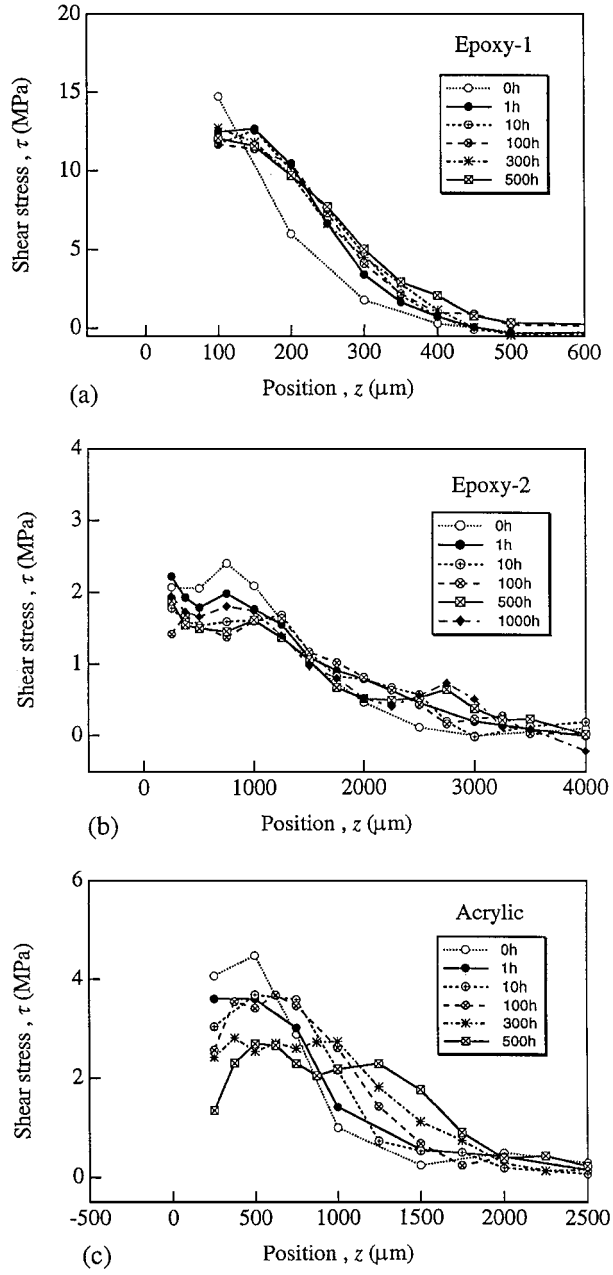

Figure 7 Profiles of interfacial shear stress in pull-out test specimens for (a) epoxy-1 matrix, (b) epoxy-2 matrix, and (c) acrylic matrix.

fiber/matrix interface. In order to correlate the creep test results for the three resins with the matrix creep behavior in the pull-out tests, the stress level in the creep test for each resin was set equal to the magnitude of τ_{max} in the corresponding pull-out test in Fig. 7. As a result, the extent of the matrix creep in the proximity of the stress transfer region of the fiber can be evaluated in an averaged sense as explained in Section 4.1.

The results of the creep tests are shown in Fig. 8 for the three resins. It is seen that epoxy-1 shows no profound creep throughout the test period. Epoxy-2 exhibits a certain amount of transient creep in an early stage, which subsequently decelerates. Acrylic undergoes significant creep which progresses in a steady manner through the entire test period.

Fig. 9 shows the results of the stress relaxation tests for the three resins at 0.5% fixed strain. The relaxation in epoxy-2 proceeds from the beginning of the test, but almost terminates in about 3 hours. Acrylic also shows

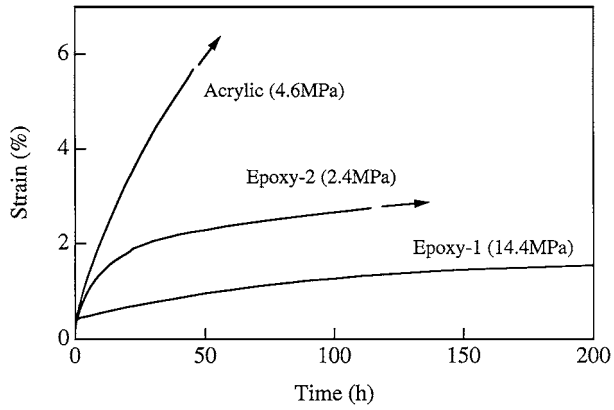

Figure 8 Tensile creep curves of matrix resins.

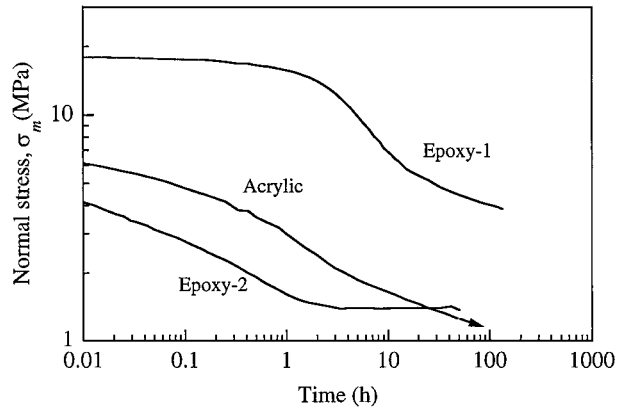

Figure 9 Stress relaxation curves of matrix resins at tensile strain of 0.5%.

relaxation in the early stage, but the stress decay in this material continues even after 20 hours. For epoxy-1, the relaxation is found to be quite slow and tends to cease after a while as with epoxy-2. These characteristics are in accord with the results of the creep tests.

4. Discussion

4.1. Influence of matrix creep

In the present study, the tensile creep tests were carried out for the three resins instead of shear creep tests, which would be more relevant to the pull-out process. The tensile stress σ in the creep test for each resin was equated to the maximum of shear stress, τ_{max}, observed in the corresponding pull-out test. Kitagawa *et al.* [14] showed experimentally that there was a certain equivalent relation, such as Tresca or Mises, between tension and shear for the inelastic deformation behavior of polyethylene and polypropylene. Their study suggests that a similar equivalence also holds between the tensile and shear creep for the resins discussed here. If a simple criterion of the Tresca type is invoked, the tensile creep tests in Fig. 8 can be regarded as response under a shear stress of $\tau = \sigma/2$ with σ chosen to be equal to τ_{max} (see Section 3.2). Accordingly, the present tensile creep tests reflect the averaged shear creep behavior in the matrix in the neighborhood of the fiber/matrix interface with shear stress distributed from τ_{max} to zero.

The above results enable a qualitative interpretation of the pull-out test results in terms of matrix creep behavior. First, in the case of epoxy-1 matrix, the shear stress at fiber/matrix interface does not generate profound creep in the matrix, and the stress profile along fiber varies little with time. In the case of epoxy-2, the matrix creeps somewhat noticeably in an early stage, resulting in a certain time variation in the fiber stress profile. However, this matrix subsequently exhibits creep hardening, which slows the creep strain rate and decelerates the change in fiber stress profiles. Finally, where acrylic is used as the matrix, immediate creep deformation occurs with less creep hardening. As a consequence, the fiber stress profile continues to change throughout the entire loading process.

The above reasoning explains fairly well the major time-dependent characteristics observed in the pull-out tests, except for the change in the epoxy-1 specimen during the initial one-hour period. For this time interval, according to the creep results in Fig. 8 the epoxy-1 matrix appears to show no significant creep. The change observed for this short duration in this specimen is considered to be the result of an interface slip due to high-shear stressing. On the whole, the present set of experiments verifies that the time-dependent change in fiber stress profiles is highly influenced by the matrix creep characteristics.

4.2. Effect of interfacial slip

Finally, attention must be paid to the effect of interfacial slippage on the time variation in fiber stress profiles in the pull-out tests. Lifshitz and Rotem [1] achieved an approximate solution to the time-dependent change in fiber stress profiles for a broken fiber in a linearly viscoelastic matrix, assuming perfect bonding at the fiber/matrix interface. When their solution is applied to the present case of a constant-load pull-out test, it implies that the stress transfer length grows on a scale of the square root of $J(t)$, where $J(t)$ represents the shear creep function of the matrix. According to this finding and with reference to the creep results in Fig. 8, the time variation in fiber stress profiles should be much greater than that observed experimentally as shown in Fig. 5. For example, in Fig. 8, after a 100-hour creep, epoxy-2 exhibits 13 times the strain as in the instantaneous value. Thus according to the theory, the stress transfer length in the corresponding pull-out test should be about 3.6 times as long after the same period, which is far beyond the actual observation.

A major source of the above discrepancy lies in the assumption of interface bonding. According to the elastic shear-lag model assuming perfect bonding [15], the maximum interfacial shear stress in the pull-out tests is given by

$$\tau_{max} = \sigma_0 \left[\frac{G_m}{2E_f \ln(R/r_f)} \right]^{1/2}, \qquad (3)$$

where G_m and E_f are the shear modulus of matrix materials and Young's modulus of fibers, respectively, and R/r_f denotes the ratio between the fiber radius and the radial distance where the matrix shear strain becomes negligible. When R/r_f is taken to be 4 in the

TABLE III Comparison of theoretical (based on perfect interfacial bonding) and experimental results on maximum interfacial shear stress τ_{max} immediately after loading

τ_{max}	Carbon fiber/ epoxy-1	Carbon fiber/ epoxy-2	Carbon fiber/ acrylic
Theoretical (MPa)	80.1	44.2	55.2
Experimental (MPa)	14.7	2.4	4.5

spirit of Li and Grubb [15], substitution of the material constants of Table I into Equation 3 yields τ_{max} for the three specimens as shown in Table III, in comparison to those measured experimentally at the moment of loading. Table III shows that the theoretical values by Equation 3 are substantially higher than those found experimentally, which is considered to be due to instantaneous interfacial slipping or shear yielding in the matrix. The experimental profiles of interfacial shear stress τ just after the moment of loading for epoxy-2 and acrylic exhibit certain extrema as already described. As a result of previous Raman spectroscopy and polarization measurements [12], such extremum points were reported to be an indication of interfacial slippage. Furthermore, there is also the likelihood of an interfacial slip in the epoxy-1 specimen, accounting for the interfacial shear stress for slipping in similar epoxy resins found to be about 20 MPa in foregoing studies [10, 12]. Since the occurrence of interface slippage suppresses the growth of interface shear stress, the creep rate of the matrix is reduced. Thus, the time variation in fiber stress profiles takes place much slower than that predicted by the approximate solution of Lifshitz and Rotem [1]. In other words, a theory based on perfect interface bonding tends to overestimate the time-dependent change in the stress transfer length in the present pull-out tests. Recently, a theoretical examination to be reported elsewhere [16] has been made of the stress profile variation in the present acrylic matrix pull-out specimen, taking into account possible interface slippage.

5. Conclusions

In the present study, constant-load pull-out tests were carried out on single-fiber model composite specimens for 500 to 1,000 hours in order to investigate the influence of matrix creep on the evolution of stress recovery length in unidirectional continuous fiber-reinforced composites. Three resins of different creep characteristics used as matrix materials were normal epoxy (epoxy-1), a blend with a more flexible epoxy (epoxy-2), and UV-curable acrylic. Single-fiber model specimens were manufactured using these resins and single carbon fibers. The time-dependent change in fiber stress profiles in the pull-out tests was measured using Raman spectroscopy, and creep and relaxation tests for the matrix resins themselves were also performed. Major findings of the present study can be summarized as follows.

1. The normal epoxy specimen did not show any notable change in the fiber stress profile after 500 hours of constant-load pull-out process. In the blended specimen with more flexible epoxy, a certain amount of growth in stress transfer length was observed for 10 hours after loading. In contrast, the specimen with a UV-curable acrylic matrix exhibited profound change in the fiber stress profile from the moment of loading to 500 hours of elapsed time.
2. The above results for constant-load pull-out tests are in fair accord with the creep and relaxation tests performed for matrix resins, which implies that the time-dependent evolution of the stress transfer length can be well correlated with the shear creep behavior of the matrix.
3. A certain indication of the occurrence of interfacial slippage was found in the present pull-out tests. Therefore, a theoretical model based on the assumption of perfect bonding at fiber/matrix interface can significantly overestimate the time-dependent change in the stress transfer length.

References

1. J. M. LIFSHITZ and A. ROTEM, *Fiber Sci. Technol.* **3** (1970) 1.
2. S. L. PHOENIX, P. SCHWARTZ and H. H. ROBINSON IV, *Compos. Sci. Technol.* **32** (1988) 81.
3. H. OHTANI, S. L. PHOENIX and P. PETRINA, *J. Mater. Sci.* **26** (1991) 1955.
4. D. C. LAGOUDAS, C.-Y. HUI and S. L. PHOENIX, *Int. J. Solids Struct.* **25** (1989) 45.
5. D. D. MASON, C.-Y. HUI and S. L. PHOENIX, *ibid.* **29** (1992) 2829.
6. K. W. KELLY and E. BARBERO, *ibid.* **30** (1993) 3417.
7. Z.-Z. DU and R. M. MCMEEKING, *J. Mech. Phys. Solids* **43** (1995) 701.
8. N. IYENGAR and W. A. CURTIN, *Acta Mater.* **45** (1997) 3419.
9. N. OHNO and T. MIYAKE, *Int. J. Plasticity* **15** (1999) 167.
10. T. MIYAKE, T. YAMAKAWA and N. OHNO, *J. Mater. Sci.* **33** (1998) 5177.
11. J. S. THOMSEN and R. PYRZ, *Compos. Sci. Technol.* **59** (1999) 1375.
12. A. K. PATRIKIS, M. C. ANDREWS and R. J. YOUNG, *ibid.* **52** (1994) 387.
13. X.-H. GU, R. J. YOUNG and R. J. DAY, *J. Mater. Sci.* **30** (1995) 1409.
14. M. KITAGAWA, T. ONODA and K. MIZUTANI, *ibid.* **27** (1992) 13.
15. Z.-F. LI and D. T. GRUBB, *ibid.* **29** (1994) 189.
16. N. OHNO, T. ANDO, T. MIYAKE and S. BIWA, *Int. J. Solids Struct.* **39** (2002) in press.

Received 11 October 2000
and accepted 25 July 2001